

On the use of dual-polarized multi-angular observations of P-band brightness temperature for soil moisture profile retrieval in thawed mineral soil

Konstantin V. Muzalevskiy, Jeffrey P. Walker, Foad Brakhasi, Nan Ye, Xiaoling Wu & Xiaoji Shen

To cite this article: Konstantin V. Muzalevskiy, Jeffrey P. Walker, Foad Brakhasi, Nan Ye, Xiaoling Wu & Xiaoji Shen (2024) On the use of dual-polarized multi-angular observations of P-band brightness temperature for soil moisture profile retrieval in thawed mineral soil, International Journal of Remote Sensing, 45:5, 1498-1521, DOI: [10.1080/01431161.2024.2313993](https://doi.org/10.1080/01431161.2024.2313993)

To link to this article: <https://doi.org/10.1080/01431161.2024.2313993>



Published online: 19 Feb 2024.



Submit your article to this journal [↗](#)



View related articles [↗](#)



View Crossmark data [↗](#)



On the use of dual-polarized multi-angular observations of P-band brightness temperature for soil moisture profile retrieval in thawed mineral soil

Konstantin V. Muzalevskiy^a, Jeffrey P. Walker^b, Foad Brakhasi^b, Nan Ye^b, Xiaoling Wu^b and Xiaoji Shen^c

^aLaboratory of Radiophysics of the Earth Remote Sensing, Kirensky Institute of Physics Federal Research Center KSC Siberian Branch Russian Academy of Sciences, Krasnoyarsk, Russia; ^bDepartment of Civil Engineering, Monash University, Clayton, Australia; ^cYangtze Institute for Conservation and Development, Hohai University, Nanjing, China

ABSTRACT



This article investigated the possibility of remotely sensing the soil moisture profile in thawed soil from multi-angular dual-polarized brightness temperature (TB) observations at P-band frequencies of 750 MHz and 409 MHz using a modified Burke model. Moreover, it was found that an excellent agreement (coefficient of determination $R^2 = 0.999$ and root-mean-square error (RMSE) no more than $RMSE = 0.6$ K) could be achieved between the Njoku coherent brightness temperature model and the modified Burke model by introducing a reflectivity from the air-soil interface that takes into account the phases of the multiple re-reflected waves in the underlying layers. Based on the modified Burke model, the depths from which apparent moisture and temperature could be retrieved in a dielectrically-inhomogeneous, non-isothermal soil were investigated, being approximately ten times less than the depth for which apparent soil temperature could be retrieved. In general, the thickness of the emitting layer depends on the TB look angle and polarization, along with the moisture and temperature profiles of the soil. It was also shown that due to the effect of the Brewster angle, the H-polarization of TB was twice as sensitive (4 K/1%) to changes in volumetric soil moisture than V-polarization (1.9 K/1%). Based on multi-angular (10° – 50°) observations of TB at H- and V-polarizations, a method of moisture profile retrieval in the top 5–15 cm soil (depending on surface moisture) was proposed using an exponential fitting function, the parameters of which are found in the course of solving the inverse problem. A decrease in the sensing frequency from 750 MHz to 409 MHz makes it possible to increase the accuracy of soil moisture profiles retrieval by a factor of two, being from $RMSE = 1.6\%$ ($R^2 = 0.946$) to $RMSE = 0.85\%$ ($R^2 = 0.982$) in the top 15 cm layer of soil. The conducted investigation shows the promise of using P-band observations of TB for soil moisture profile retrieval.

ARTICLE HISTORY

Received 5 July 2023
Accepted 26 January 2024

KEYWORDS

Microwave remote sensing; radiometry; P-band; Burke model; moisture and temperature retrieval depth; soil moisture profile

CONTACT Konstantin V. Muzalevskiy  rsdkm@ksc.krasn.ru  Laboratory of Radiophysics of the Earth Remote Sensing, Kirensky Institute of Physics Federal Research Center KSC Siberian Branch Russian Academy of Sciences, Krasnoyarsk, Russian Federation

1. Introduction

At present, the lowest frequency satellite soil moisture products on a global scale are based on NASA's Soil Moisture Active-Passive (SMAP) (Entekhabi et al. 2014) and ESA's Soil Moisture and Ocean Salinity (SMOS) (Kerr et al. 2001) radiometric data at a frequency of 1.4 GHz (L-band). For 1.4 GHz, the depth of soil moisture retrieval is usually determined in the range from about 1.0–5.0 cm (Entekhabi et al. 2014; Escorihuela et al. 2010; Newton et al. 1982; Schmugge 1980; Schmugge et al. 1976; Schrnugge and Choudhury 1981; Shen et al. 2021; Wang and Choudhury 1980). The use of lower frequency radiometers (at 750 MHz) can increase the sensing depth (depth of soil moisture retrieval) to 10.5 cm and reduce the impact of soil surface roughness, as well as the wave scattering on the elements of vegetation cover (Shen et al. 2021).

Experimentally, the depth of soil moisture retrieval is determined by correlation between the observed brightness temperature (TB), emissivity or polarization index with averaged soil moisture measured in the top soil layer of different thicknesses. However, the radiative transfer model (Stogryn 1970) shows that the soil moisture and temperature profiles have independent effects on the brightness temperature (E. G. Njoku, Schiedge, and Kahle 1980, 20–22). Accordingly, Shen et al. (2021) showed that the moisture retrieval depth can be determined through equality of the emissivity of a heterogeneous soil and the Fresnel emissivity, calculated for the average moisture of the layer of desired thickness. A similar approach to determining the moisture retrieval depth in the P-band was used in Muzalevskiy (2021) based on calculation of radar backscatter coefficient. Much earlier, the idea of estimating the equivalent moisture in a desired thickness of top soil was proposed in Newton et al. (1982, see Equation (1)).

Shen et al. (2021) made a theoretical study of moisture retrieval depth as a function of frequency (300 MHz to 10 GHz) on model soil moisture profiles with a soil clay fraction of 10.9% and a density of $0.87 \text{ g}\cdot\text{cm}^{-3}$ at a look angle of 30° with H-polarization. They showed that moisture retrieval depth depends on both frequency and soil moisture profile shape, with a moisture retrieval depth varying from 0.8 cm to 10.5 cm at 750 MHz, and from 0.6 cm to 8.4 cm at 1.4 GHz. Moreover, experimental data showed that correlations between the microwave polarization difference index and the soil moisture content averaged over different soil thicknesses showed a larger moisture retrieval depth at 750 MHz (~ 7 cm) than at 1.4 GHz (~ 5 cm) (Shen et al. 2021), and that this varied according to the top soil moisture gradient, in addition to the average soil moisture content.

Ongoing research by Brakhasi et al. (2023) has demonstrated the possibility of combining single or dual-frequency (L-band/P-band), single or dual-polarization (H-pol/V-pol), single or multi-incidence angle (40° and 46° for P-band/ 38° and 45° for L-band) brightness temperature measurements for soil moisture profile retrieval. They found from a numerical experiment that combined L-band and P-band observations outperformed the other combinations tested. RMSE of volumetric soil moisture retrieval was less than 4% (here and everywhere below % v/v) for depths up to 28 cm for a dry period, but only to 5 cm for a wet period. Results were further confirmed experimentally, showing that the accuracy of soil moisture profile retrieval using dual-polarized dual-frequency brightness temperature measurements at one incidence angle (40°) outperformed using multi-incidence angles at L-band or P-band alone (Brakhasi et al. 2023).

Coherent models have been developed to calculate the brightness temperatures of an inhomogeneous non-isothermal half-space, based on the fluctuation-dissipation theorem (Landau and Lifshitz 1960; Rytov 1953). These models take into account the local attenuation of the auxiliary wave in each of the layers of a medium during multiple reflections of the wave (with phases) in all upper-lying and lower-lying layers (Klepikov and Sharkov 1983; E. Njoku and Kong 1977; Stogryn 1970; Tsang, Njoku, and Kong 1975; Wilheit 1978). Non-coherent radiative transfer models (Liu et al., 2013; Burke, Schmugge, and Paris 1979; Shulgina 1975; Tsang and Kong 1975) have also been developed in which emissivity is determined by the dielectric contrast at the air/soil interface alone. These models are widely used to calculate TB of soils (Entekhabi et al. 2014; Kerr et al. 2001). However, incoherent models (eg. Burke, Schmugge, and Paris 1979) can lead to a substantial difference (up to 20 K) in the prediction of brightness temperatures relative to coherent models at 1.4 GHz (E. Njoku and Kong 1977; Wilheit 1978) in the case of moisture profiles with a steep gradient near the surface.

In this paper, a modification of the incoherent Burke model (Burke, Schmugge, and Paris 1979) is proposed, which allows the emissivity to be calculated taking the layered structure of the underlying soil layers into account by applying the Brekhovskikh method (Brekhovskikh 1960). This makes it possible to achieve a TB modelling accuracy close to that of the coherent Njoku model (E. Njoku and Kong 1977). Accurate coherent models are based on a cumbersome nonlinear iterative scheme, in which all the elements of propagation matrix (Tsang, Kong, and Ding 2000, see 5.2.2) should be calculated for each boundary in the layered inhomogeneous half-space. The proposed modification of the incoherent Burke model, referred to herein as the modified Burke model, will not only improve its accuracy, but also allow for using a simpler iterative algorithm, in which the reflectivity of the inhomogeneous half-space is calculated only once for the air-soil interface. Based on the modified Burke model, the effect of moisture and temperature profiles on TB and the subsequent soil moisture retrieval depth as a function of moisture and temperature profiles was investigated. Consequently, a method was proposed for moisture profile retrieval of a drying soil based on dual-polarized multi-angular observation of TB at P-band, including at 750 MHz and 409 MHz (which is reserved for radio astronomy purposes in the range of 406.1–410 MHz).

2. Approximate coherent TB model of layered-non-isothermal soils

According to the incoherent Burke emission model (Burke, Schmugge, and Paris 1979), the TB of a layered inhomogeneous non-isothermal half-space with a smooth surface can be calculated using the radiative transfer equation (Chandrasekhar 1950). By dividing the layered inhomogeneous half-space (continuous vertical profile of the relative complex permittivity (RCP) and temperature) into n partial layers of thickness Δz , and taking into account the radiation emitted within the k^{th} layer together with upwelling radiation from the bottom boundary of each layer, the brightness temperature T_b can be calculated by iteration using (Burke, Schmugge, and Paris 1979)

$$Tb_{p,k} = T_{s,k}(1 - \gamma_k)(1 + \gamma_k \Gamma_{p,k}) + Tb_{p,k+1} \gamma_k (1 - \Gamma_{p,k}). \quad (1)$$

The iterative process starts from the bottom layer $k=n, \dots, 0$, $Tb_{p,n+1} = T_{s,n+1}$, $\Gamma_{p,n}$ is the reflectivity from the boundary between n and $n+1$ layers. Here, $T_{s,k}$ is the physical temperature of the soil in the k^{th} layer; $\gamma_k = \exp(-2k_0 \cdot \Delta z \cdot \kappa_{s,k} / \cos \theta^t_k)$, θ^t_k is the wave refraction angle at the interface between the partial layers k and $k+1$; k_0 is the wave number in free space; $\kappa_{s,k}$ is the normalized attenuation coefficient in k^{th} layer; $\kappa_{s,k} = \text{Imag} \sqrt{\epsilon_s(z_k)}$, $z_k = k \cdot \Delta z$; $\epsilon_s(z_k)$ is the RCP of the soil at depth z_k . In Equation (1), each of the reflectivities $\gamma_{p,k}$ are local and do not take into account the layered structure of the half-space medium above k or below $k+1$ boundaries, and also does not take into account wave re-reflections (with phase) inside the layer between these boundaries. Such assumptions can lead to an error in the calculation of TB from 3 K to 20 K at a frequency of 1.4 GHz when compared to the coherent Njoku (E. Njoku and Kong 1977) or Wilheit (Wilheit 1978) model. As frequency decreases, this error increases (E. Njoku and Kong 1977, see Figure 13). However, the accuracy of Equation (1) can be substantially improved by calculating the reflectivity at the air-soil surface boundary $\gamma_{p,1}$ using the complex reflection coefficient from a layered inhomogeneous half-space according to the Brekhovskikh method (Brekhovskikh 1960, see Equation 5.48, 5.49), which takes into account the multi-reflection of the wave in terms of phase and amplitude from each of the underlying layers.

The error of the modified (coherent) Burke model can be estimated with respect to the known exact coherent Njoku model and experimental data. Accordingly, TB was first calculated as a function of frequency from 100 MHz to 10 GHz for nadir observations of a layered soil for six moisture profiles and one temperature profile (profile 6) according to Njoku and Kong (1977, see Figures 10 and 12). Accordingly, their moisture and temperature profiles are reproduced in Figure 1. Soil RCP (Zaneis loam) was calculated based on the Wang and Schmugge (1980) model for sand, silt, and clay content of 48.0%, 36.0%, and 16.0%, respectively. Figure 2 presents the comparison results of TBs calculated using the modified and incoherent Burke model, and the exact coherent Njoku model, showing a very good agreement between the modified Burke model and the exact coherent Njoku model over the entire frequency range under study. The incoherent Burke model (see Figure 2(a), dash lines) showed good agreement with the Njoku model only for moisture profile 1 (high soil moisture with small moisture gradient) and profile 4 (dry soil with small moisture gradient) at frequencies above 200 MHz. For the rest of the moisture profiles, the incoherent Burke model had a satisfactory agreement with the Njoku coherent model only at frequencies above ~ 1 GHz. Note that the modified Burke model well described the phenomenon of TB interference observed for moisture profile 6 (see Figure 1). In general, the modified Burke model in the frequency range from 100 MHz to 10 GHz produced a coefficient of determination of $R^2 = 0.999$ and $\text{RMSE} = 0.6\text{K}$ (see Figures 2(b)), and so accurately described the TBs calculated using the coherent Njoku model.

A comparison is also made in Figure 3 between TB calculations from the modified Burke model, incoherent Burke model, and coherent Njoku model when viewing from nadir or at 60° for V-polarization, with various combinations of the temperature and moisture profiles given in Figure 1. The comparison was made at a frequency of 750 MHz, which has recently been used in theoretical and experimental studies (Brakhasi et al. 2023; Shen et al. 2021, 2022a, 2022b; Ye et al. 2021). Both the incoherent and modified

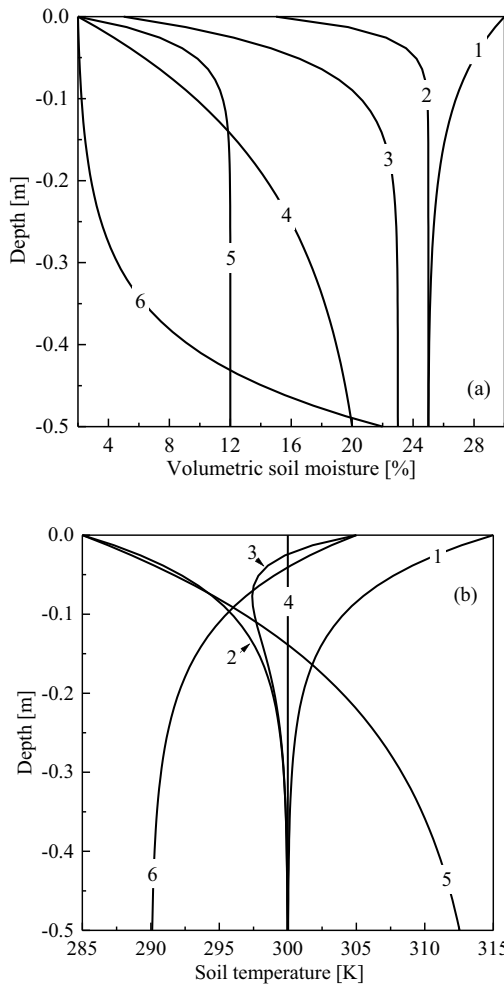


Figure 1. Approximation to (a) moisture and (b) temperature profiles measured under natural conditions (E. Njoku and Kong 1977).

Burke models were found to be highly correlated with the coherent Njoku model. However, the modified Burke model had a lower RMSE (0.4 K) than the incoherent Burke model (5.7 K) relative to the coherent Njoku model (see Figure 3).

Testing was also undertaken on a layered inhomogeneous non-isothermal half-space given in the form (Tsang, Kong, and Ding 2000, see text to Figure 5.2.7)

$$\epsilon(z) = \begin{cases} \epsilon(z) = 1 & z < 0\text{cm} \\ \begin{cases} \epsilon(z) = (3 + i0.3)\exp[-0.06z] \\ T_s(z) = 280 \pm 20\exp[0.1z] \end{cases} & -30 < z \leq 0\text{cm} \\ \begin{cases} \epsilon(z) = \epsilon(z = -30) \\ T_s(z) = T_s(z = -30) \end{cases} & z \leq -30\text{cm}. \end{cases} \quad (2)$$

The calculation results based on the modified Burke model and the coherent Njoku model for the layered structure in Equation (2) are presented in Figure 4, with a good agreement between the models between 100 MHz and 10 GHz. The RMSE and R^2 between the

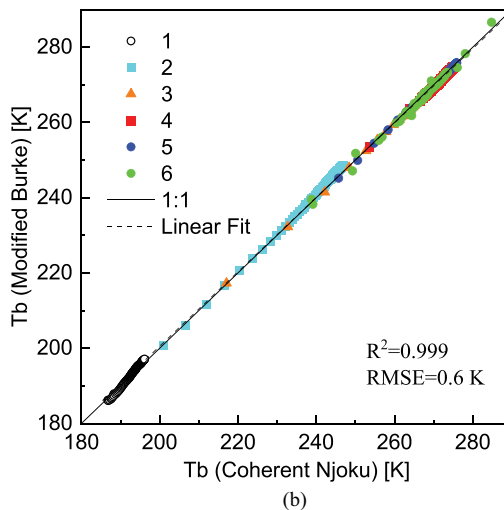
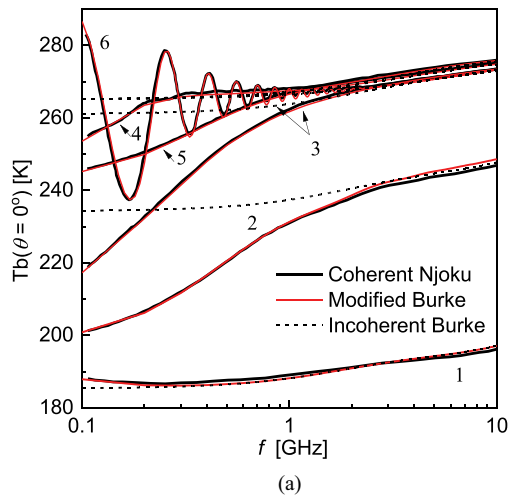


Figure 2. (a) Brightness temperature observed at nadir, calculated by three models for six moisture profiles (see Figure 1(a)) and one temperature profile (see Figure 1(b), profile 6). The solid black lines represent the results of calculations (Tsang, Kong, and Ding 2000, see figure 5.4.8) using the coherent Njoku model (E. Njoku and Kong 1977). Dashed lines of different colours indicate calculations with the incoherent Burke model (Burke, Schmugge, and Paris 1979). Solid red lines correspond to calculations based on the modified Burke model. (b) Correlation between brightness temperature calculated from the modified Burke model and coherent model in all frequency range. Symbols indicate the soil moisture profile number (see Figure 1(a)).

brightness temperature calculated using the coherent Njoku model and the modified Burke model were calculated as 0.14 K and 0.999, respectively.

A final evaluation is given in Figure 5, showing a time series comparison of the experimental data measured at 750 MHz and viewing angle of 46° by Brakhasi et al. (2023, see Figure 2(a–c)) (Period A, Station 126) with brightness temperature calculated by the modified Burke model. In this calculation, Equations (7) and (8) from Brakhasi et al. (2023) were used to take the roughness of the soil surface into account with the

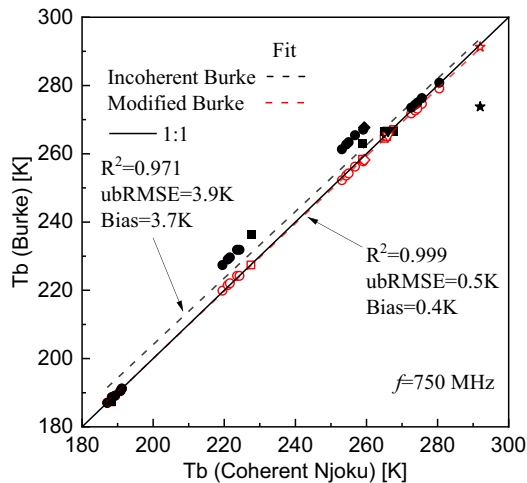


Figure 3. Comparison of brightness temperatures calculated for nadir sensing (except for the asterisk which is at a 60° looking angle, vertical polarization) based on the incoherent Burke model (Burke, Schmugge, and Paris 1979) and the modified Burke model relative to the coherent Njoku model (E. Njoku and Kong 1977) at 750 MHz. Filled black symbols are the incoherent Burke model and open red symbols are the modified Burke model. Circles are data from Njoku and Kong (1977, see figure 14), squares are data from Tsang et al. (2000, see figure 5.4.8), diamonds, triangles, and asterisk is data from Njoku and Kong (1977, see figure 13a, 13b-normal incidence, 13b-vertical polarization, respectively).

corresponding published parameters. The Mironov et al. (2013) model was used to calculate the complex permittivity. The modified Burke model produced a $R^2 = 0.937$ and $RMSE = 4.2$ K for both H- and V-polarization (see Figures 5).

3. Influence of moisture and temperature profiles on the angular dependences of TB. The layer of soil that forms TB

Based on the modified Burke model using the Mironov et al. (2013) dielectric model for soil with a clay content $C = 21\%$ (by weight) and a dry bulk density $\rho_d = 1.1 \text{ g}\cdot\text{cm}^{-3}$, the angular dependences of TB was calculated at a frequency of 750 MHz (see Figure 6) for moisture profiles W_{1-4} and temperature profiles $T_{s1,2}$ (see Figure 1). It can be seen from Table 1 (calculated based on Figure 6) that H-polarization was two times more sensitive to volumetric soil moisture variations (4 K/1%) than V-polarization (1.9 K/1%). This was especially noticeable when comparing pairwise V- and H- polarizations for moisture profiles W_3 and W_4 (see Figure 6), which differed in surface soil moisture by 3%. It can also be seen that the TB values practically coincided for V-polarization at a look angle of 55° , within their uncertainty band, for moisture profiles W_3 and W_4 (see Figure 6). In contrast, the TB values differed substantially from each other over the entire range of observation angles and moisture profiles for horizontal polarization. Moreover, for the considered moisture profiles, the 30 K increase in soil surface temperature between profiles 2 and 1 (see Figure 1(b)) resulted in a TB change in the range of 6–11 K (see Table 1), due to the fact that as the look angle increases the reflection coefficient increases at H- polarization and decreases at V-polarization. However, when approaching the

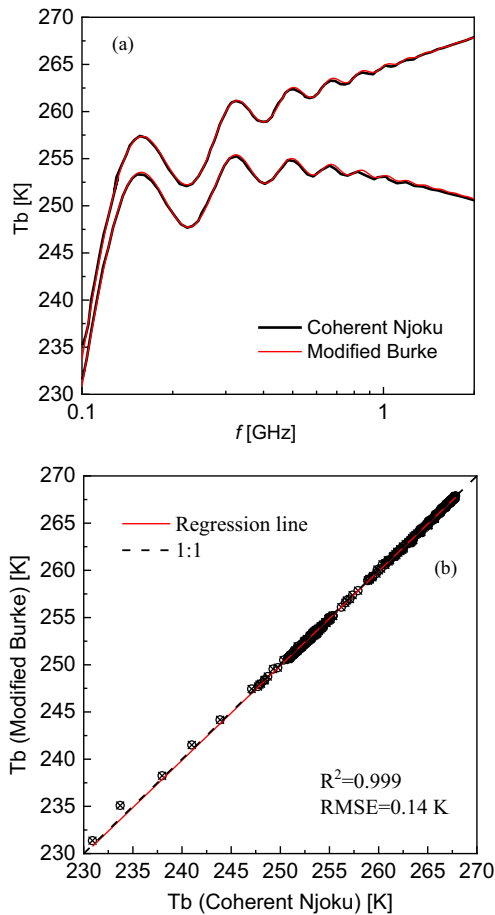


Figure 4. (a) Spectrum of brightness temperature for nadir viewing angle, calculated by the coherent Njoku model (Tsang, Kong, and Ding 2000, see figure 5.2.7) and modified Burke model between 100 MHz and 10 GHz. (b) Correlation between the brightness temperatures in all frequency range.

Brewster angle, TB is more influenced by the physical temperature of the soil at V-polarization. From the data presented in Figure 6, it can also be seen that in the range of observation angles less than 15–25°, for the same moisture profile TB at H-polarization can be greater than TB at V-polarization, depending on the physical temperature profile of the soil. The calculations show (not shown graphically in the article) that the angular dependences of the polarization index decrease by about 3 times when the soil dries up and changes from a moisture profile of W_1 to W_4 (see Table 2). This is seen in Figure 6 from the decrease in difference between the angular dependencies of TBs at V- and H-polarization.

In the range of observation angles from 10° to 55° for V- and H-polarizations, TBs were calculated depending on the thickness z_L of the soil sensing depth, along with the vertical moisture profiles W_2 , W_4 and temperature $T_{s1,2}$. Below the sensing depth thickness of z_L , the soil was considered to be a homogeneous dielectric half-space with moisture and

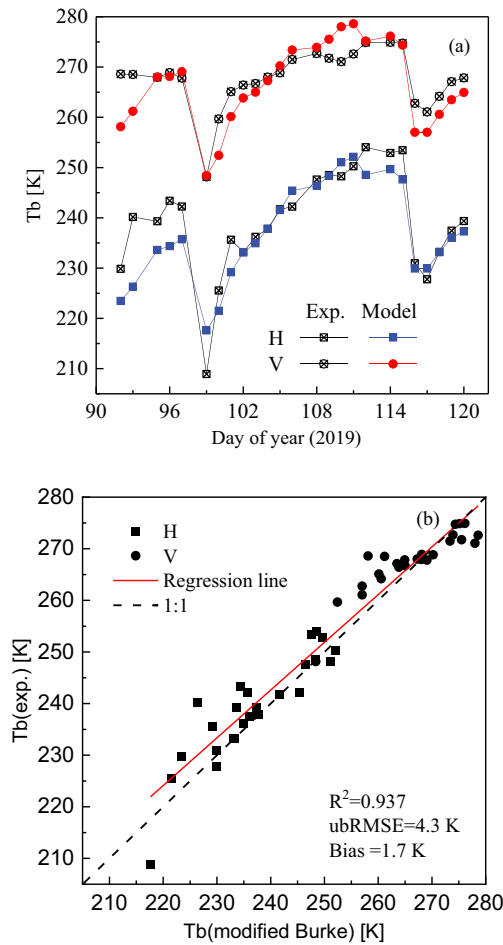


Figure 5. (a) Time series of brightness temperature measured in the PRISM experiment at 750 MHz (Brakhasi et al. 2023, see figure 2, period A) and that calculated based on the modified Burke model. (b) Correlation between the measured and calculated brightness temperatures.

temperature coinciding with the lower boundary of the layer. Calculated values of TB were then normalized to TB at a total layer thickness of $z_L = 0.5$ m and presented in Figure 7, showing that TB saturation, with increasing of the thickness of layer z_L , depends on both soil moisture and temperature profiles and on looking angle (see Figure 7, shaded bars). For moisture profiles 2–4 and temperature profiles 1–2, the thickness of the emitting layer decreased for V-polarization and increased for H-polarization with increasing observation angle. To test these patterns, similar calculations were made for moisture profiles 1–5 and temperature profiles 1 and 2. From the saturation level of 95% normalized TB (see Figure 7), the thicknesses of the emitting layer z_{eff} was determined. Note that, as a result of interference, the value $Tb_{H,V}(z_L)/Tb_{H,V}(z_L = 0.5 \text{ m})$ has the character of damping oscillation that with increasing z_L can exceed unity, as in the case of moisture profile W_2 and temperature $T_{s,1}$ profiles (see Figure 7). The thicknesses of the emitting layer z_{eff} as a function of TB viewing angle are shown in Figure 8. For all considered moisture profiles,

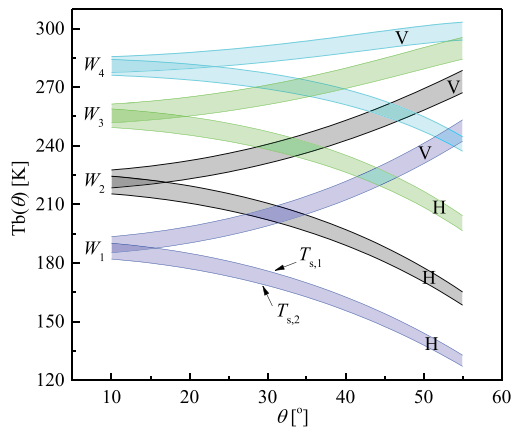


Figure 6. Angular dependences of brightness temperature at 750 MHz as calculated based on the modified Burke model for soil moisture profiles 1–4 (W_1 – W_4) (see [figure 1a](#)) at variation of soil temperature profiles from 1 to 2 ($T_{s,1}$ - $T_{s,2}$). The upper and lower boundaries of the coloured bands correspond to temperature profiles 1 ($T_{s,1}$) and 2 ($T_{s,2}$) respectively.

Table 1. Variation of brightness temperature depending on viewing angle, polarization for two contrasting moisture profiles^a.

Moisture profile	Brightness temperature [K]			
	10°		55°	
	H	V	H	V
1	182–189	185–193	127–133	242–253
4	276–283	277–286	237–245	293–303

^aWhen varying between two contrasting temperature profiles 1 and 2 (see [Figure 1\(b\)](#)).

Table 2. Angular dependences of polarization index (PI)^a.

Moisture profile	Viewing angle [°]		
	20	40	55
1	0.072	0.31	0.62
4	0.021	0.096	0.21

^aPI = $2 \cdot (Tb_V - Tb_H) / (Tb_V + Tb_H)$.

the thickness of the emitting layer increased for H-polarization and decreased for V-polarization, when increasing the look angle from 10° to 55° (see [Figure 8](#)). During the soil surface drying, the thickness of the emitting layer increased. Surprisingly, however, the thickness of the emission layer for moisture profile 5 aligned more closely with the thickness of emission layer for profile 3 rather than for profile 4 (compare moisture values at the soil surface of these profiles, see [Figure 1](#)). At the same time, the thickness of the emitting layer of wetter soil (see [Figures 1 and 7](#), profile 3) was greater than the thickness of the emitting layer of drier soil ([Figures 1 and 7](#), profile 5). This is apparently because profile 5 has a thinner transition layer than profile 3. As a result, to achieve a 95% level of the TB value (similar to the graphs shown in [Figure 7](#)), it is required to take a thicker topsoil of profile 3 than profile 5. A similar effect was noticed by Shen et al. (2021) for the moisture gradient near the soil surface on the sensing depth. It is also noted here

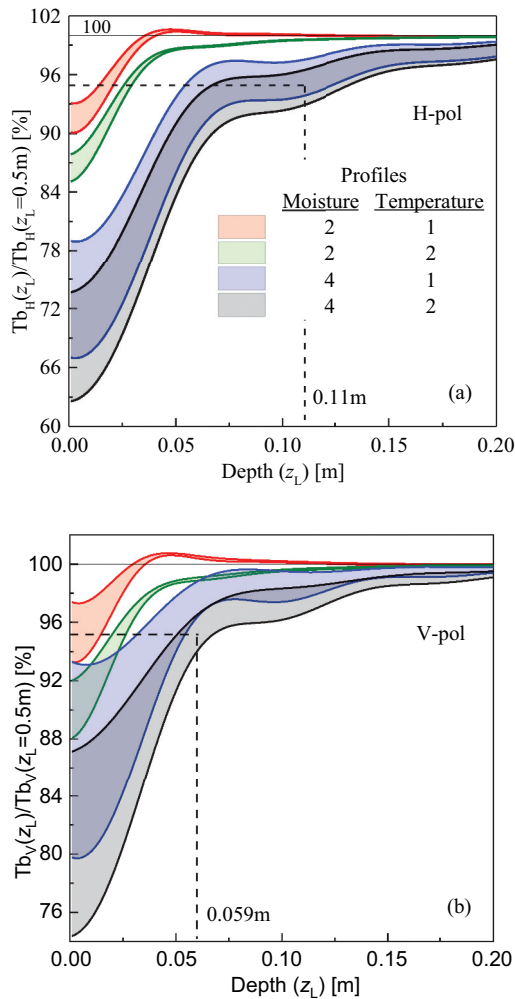


Figure 7. Normalized brightness temperature at 750 MHz calculated according to the thickness z_L of the dielectric-inhomogeneous non-isothermal layer and soil moisture and temperature profiles as indicated. (a) For H-polarization, the lower and upper boundaries of the bands correspond to the look angle of 55° and 10° , respectively. (b) For V-polarization, the lower and upper boundaries of the bands correspond to the look angle of 10° and 55° , respectively.

that for moisture profile 4, the thickness of the emitting layer at H-polarization ($z_{\text{eff}} \sim 0.11$ m) was more than 2 times higher than the thickness of the emitting layer at V-polarization ($z_{\text{eff}} \sim 0.059$ m) with increasing looking angle (see Figures 7 and 8). The variation of temperature profile from profile 1 to profile 2, on average for all moisture profiles, had a moderate effect on the thickness of the emitting layer (about 10% of the average level). Substantial variations in the thicknesses of the emitting layers, depending on the moisture profiles and TB looking angle, make it possible to propose a method for moisture profile retrieval from observations of multi-angular H- and V-polarized TB.

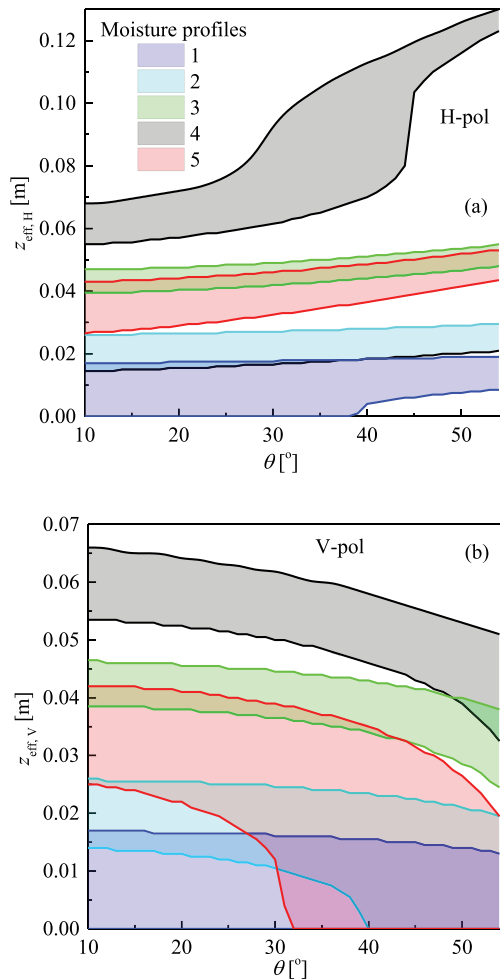


Figure 8. Thickness of emitting layer depending on look angle and polarization of brightness temperature at 750 MHz for soil moisture profiles 1 to 5 and temperature profiles 1 and 2, with the lower and upper boundaries of the coloured bands corresponding to temperature profiles 1 and 2, respectively.

4. Soil moisture profile retrieval from dual-polarized multi-angular TB observations

To investigate the possibility of remotely sensing the soil moisture profile, the moisture profiles of Schmugge et al. (1976) have been used, observed over a 37-day period from 2 March 1971 (see Figure 9). Soil moisture profile 1 was not presented in Schmugge et al. (1976, 1981), so it was derived herein using two-dimensional interpolation (over depth and time). The temperature profiles between day 1 and day 2 were also missing, they were taken as for day 3.

4.1. Apparent moisture and temperature retrieval of stratified non-isothermal soil

The TB of a dielectrically homogeneous isothermal half-space of bare soil with a flat boundary can be calculated using (Ulaby et al. 2014, see p. 556)

$$Tb_p^{hom}(\theta, W, T_s) = [1 - \Gamma_p(\theta, W)]T_s, \quad (3)$$

where T_s is the physical temperature of soil and index p stands for H- and V-polarizations, $\Gamma_p(\theta, W)$ is the Fresnel reflectivity from a homogeneous soil with volumetric moisture of W . Calculations of reflectivity at a frequency of 409 MHz and 750 MHz at angle $\theta = 0^\circ$ showed that an increase in soil temperature from $T_s = 10^\circ\text{C}$ to $T_s = 40^\circ\text{C}$ leads to an increase in reflectivity of no more than 0.6 dB at $W \sim 6\text{--}10\%$ and less than 0.3 dB at $W > 20\%$. In these calculations, the dielectric model of Mironov et al. (2020) was used, with clay weight fraction and dry bulk density taken equal to 5–21% and $1.2 \text{ g}\cdot\text{cm}^{-3}$ respectively. Therefore, the temperature dependence of RCP in $\Gamma_p(\theta, W)$ is neglected. The angular values of TB were then calculated for V- and H-polarizations using the modified Burke model $Tb_p^{\text{Burke}}(\theta, W_j(z), T_{s,j}(z))$ for moisture profiles $W_j(z)$ and temperature $T_{s,j}(z)$, where z is the vertical coordinate (measured from the surface to the depth of the soil), and the index j runs through all profile numbers (see Figure 9). The inverse problem of finding the apparent moisture W and temperature T_s of an equivalent dielectrically homogeneous, isothermal half-space can then be solved from

$$\{W, T_{s,j}\} = \min \left\{ \sum_{p,\theta} \left| Tb_p^{hom}(\theta, W, T_s) - Tb_p^{\text{Burke}}(\theta, W_j(z), T_{s,j}(z)) \right|^2 \right\}. \quad (4)$$

This minimization problem was solved using the Levenberg-Marquardt algorithm (Gill and Murray 1978) at both polarizations simultaneously for the range of viewing angles from 10° to 50° with a 5° step. When calculating TB, the Mironov two-relaxation refractive RCP model (L. Mironov, Bobrov, and Fomin 2013) was used. Clay content (by weight) and dry bulk density were set equal to 21% and $1.1 \text{ g}\cdot\text{cm}^{-3}$, respectively. Note that by solving the system of algebraic equations for H- and V-polarizations, an analytical expression for soil temperature can be obtained. This equation takes on a particularly simple form for a viewing angle of 45° being (Bogorodsky and Kozlov 1985)

$$T_s = Tb_H^2(45^\circ) / [2Tb_H(45^\circ) - Tb_V(45^\circ)]. \quad (5)$$

This equation does not consider the layered structure of the soil of Equation (3). The retrieved apparent temperature and moisture values of the layered non-isothermal soil according to day after irrigation are shown in Figure 10 (solid lines). For greater visibility, the direct and inverse problems were solved not only at a frequency of 750 MHz but also at a frequency of 409 MHz. The R^2 and RMSE between the apparent soil temperature from Equation (4) and the estimated value according to Equation (5) for both frequencies are within $R^2 = 0.972\text{--}0.991$ and $\text{RMSE} = 0.3\text{--}0.4 \text{ K}$. The greatest differences were observed for dry soil from approximately 12–18 days after irrigation, when the emission depth increased and the effect of deep moisture and temperature profiles had greater impact on the simulated TB. The most substantial differences (more than 1 K) between apparent soil temperatures, retrieved at 409 MHz and 750 MHz, were observed from the 16th day after irrigation (see Figure 10(a)). For all days after irrigation, apparent soil moisture values, retrieved for both frequencies (see Figure 10(b)), differ from each other by less than 4%.

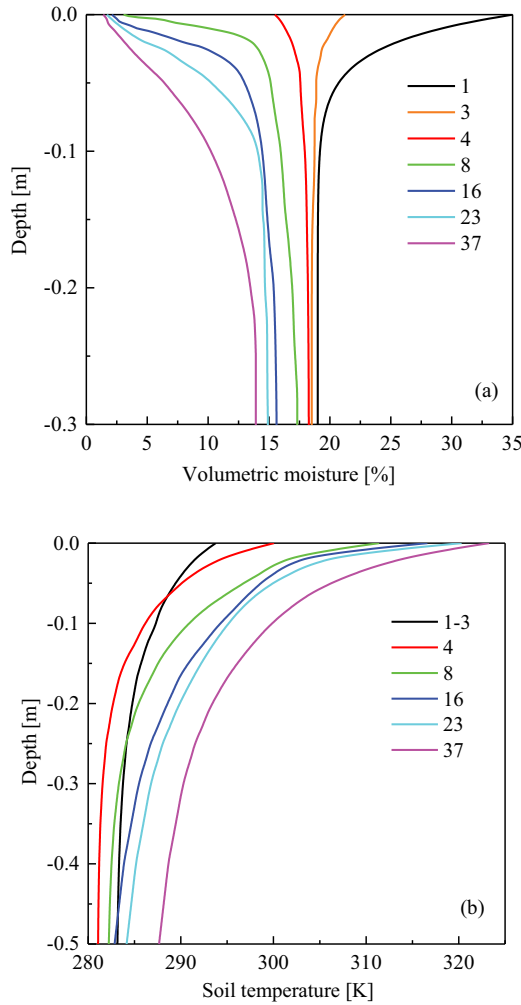


Figure 9. Experimentally measured soil moisture (a) and temperature profiles (b) for 37 days after irrigation (Schmugge et al. 1976; Schnugge and Choudhury 1981).

Interestingly, the time series of apparent soil moisture values retrieved at different frequencies intersected (see Figure 10(b)) on the day of the change in sign of the moisture profile gradient (see Figure 9(a)), which can be used to retrieve the moisture gradient near the soil surface. Although the apparent values of soil moisture and temperature were found from the brightness temperatures, it is the emissivity and effective temperature of the soil, respectively, that determine the retrieved values. This fact was previously noted Njoku et al. (1980). Considering a phenomenological model of radiation transfer for a layered-inhomogeneous non-isothermal half-space

$$Tb_p^{RT}(\theta, W_j(z), T_{s,j}(z)) = \eta_p T_{\text{eff}} \tag{6}$$

$$T_{\text{eff}} = 2k_0 \int_0^\infty dz T_{s,j}(z) K_j(W_j(z), T_{s,j}(z)) e^{-2k_0 \int_0^z K_j(W_j(\xi), T_{s,j}(\xi)) d\xi}$$

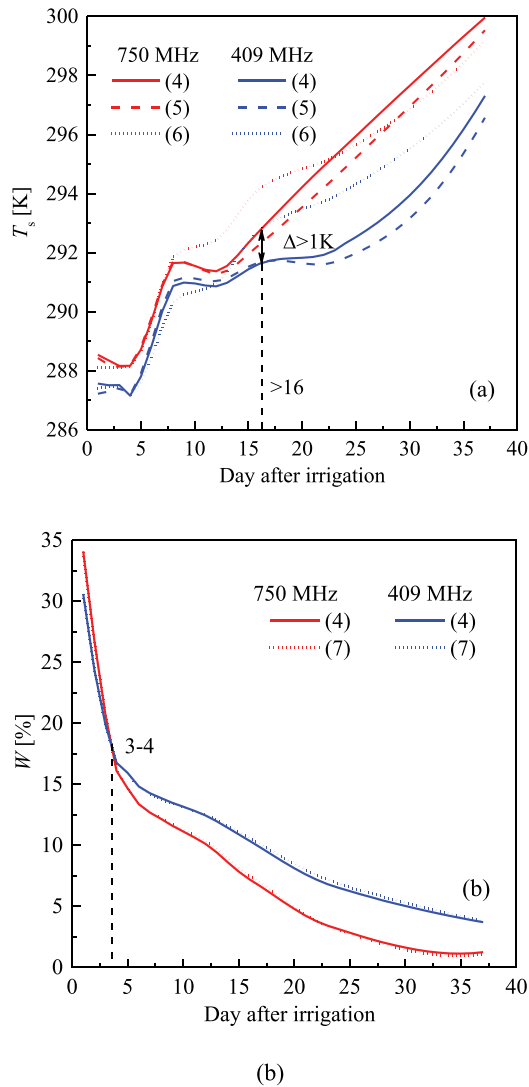


Figure 10. Calculated (a) Apparent temperature and (b) Volumetric moisture of a stratified non-isothermal soil profile at 750 MHz and 409 MHz during the 37 days post-irrigation event of [figure 9](#).

where $\eta_p = [1 - \rho(\theta, W_j(z), T_{s,j}(z))]$ is the reflectivity, calculated for a layered medium by the Brekhovskikh (1960) method. The effective soil temperature T_{eff} depends on both the temperature profile $T_{s,j}(z)$ and the moisture profile $W_j(z)$ of the soil. The values of effective soil temperature calculated based on Equation (6) are shown in [Figure 10\(a\)](#) (short dot lines). The coefficient of determination and RMSE between the soil temperature T_s obtained in the course of solving the inverse problem of Equation (4) and T_{eff} using Equation (6) for both frequencies are within $R^2 = 0.927\text{--}0.942$ and $\text{RMSE} = 0.78\text{--}0.84$ K. It can be seen that T_{eff} agrees well with the retrieved T_s values in the first days after irrigation ($<7\text{--}12$). For subsequent days, T_s deviate more from T_{eff} due to an increase in wave penetration into dry soil, the layering of which was not

considered in either Equations (3)-(5). Further, considering that the permittivity of thawed soil weakly depends on the soil temperature, then the emissivity can be considered only as a function of soil moisture. Under this assumption, an inverse problem similar to Equation (4) was solved by finding the apparent soil moisture from minimizing the norm of the discrepancy between the emissivity $\eta_p^{hom}(\theta, W)$ calculated for a dielectrically homogeneous half-space such that

$$W_j = \min \left\{ \sum_{p,\theta} \left| \eta_p^{hom}(\theta, W_j) - \eta_p(\theta, W_j(z)) \right|^2 \right\}, \quad (7)$$

with $\eta_p(\theta, W_j(z))$ from Equation (6). The apparent soil moisture found from the emissivity is shown in Figure 10(b) (short dot lines). The time series of apparent soil moisture retrieved from the TB values in the course of solving the minimization problem in Equation (4), practically coincide with the apparent soil moisture retrieved only from emissivity in Equations (7). Comparing the apparent temperature and soil moisture found in the course of minimization using Equation (4) (see Figure 10) with the average values of physical temperature and soil moisture in a layer with thickness l_{Ts} and l_W , calculated based on the corresponding profiles (see Figure 9), the effective sensing depth was estimated. Figure 11 (see dash lines) shows substantial differences between the effective depth estimates l_W and l_{Ts} . In this case, the time dependence of l_W is not monotonic, with the value of l_W beginning to decrease from day 7, and becoming almost equal to 0 after 30 days after irrigation (see Figure 11(b)) at a frequency of 750 MHz. In general, more than a two-fold increase in the depth of apparent soil moisture retrieval was observed when the frequency reduced from 740 MHz to 409 MHz (see Figure 11(b)).

Retrieval depth of apparent temperature does not change as much with decreasing frequency (see Figure 11(a)). For additional comparison, thermal skin depth l_{sd} values were estimated based on equation:

$$2k_0 \int_0^{l_{sd}} dz \kappa_j(z) = 1, \quad (8)$$

where $\kappa_j(z) = \text{Im} \sqrt{\epsilon_j(z)}$ is the normalized attenuation coefficient calculated from the dielectric model (L. Mironov, Bobrov, and Fomin 2013) for j^{th} moisture and temperature profiles (see Figure 9). During the soil drying, the thermal skin depth l_{ds} calculated based on Equation (8) correlates more with l_{Ts} than l_W (see Figure 11(a)) and has significant differences with the value of l_W .

4.2. Moisture profile retrieval for layered-heterogeneous non-isothermal soil

Integral Equation (6) says that the simultaneous retrieval of the soil moisture and temperature profiles is a non-linear ill-posed problem (the Fredholm equation of the first kind). To simplify the problem, only soil moisture profiles were retrieved. The soil temperature T_s is considered constant with a depth equal to the apparent soil temperature determined from equation (5), which as shown above, is very close to the temperature obtained from Equation (4) and the effective temperature from Equation (6). To increase the stability of an ill-posed problem solution, and paying attention to the fact that the soil moisture profiles (see Figure 9(a)) are close to an exponential function in the top soil layer,

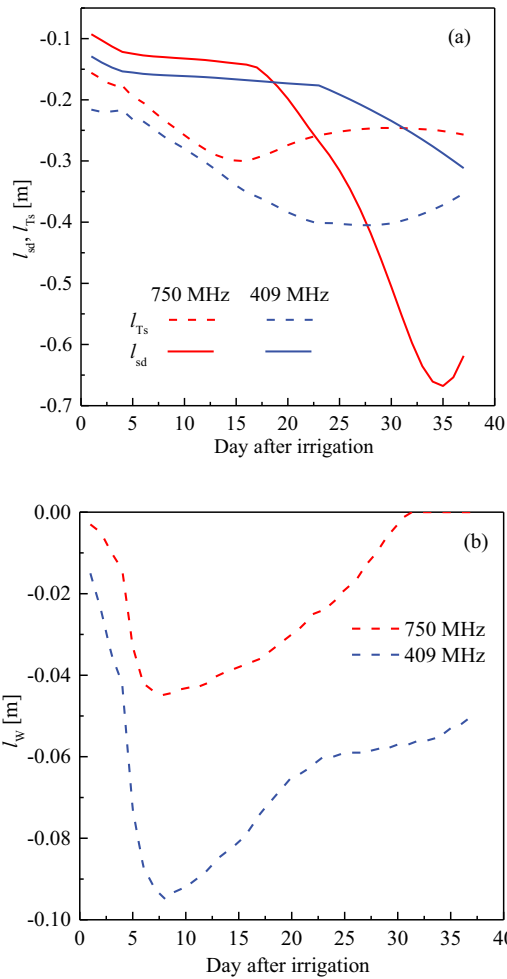


Figure 11. (a) Thermal skin depth l_{sd} and apparent temperature l_{Ts} , and (b) moisture l_w retrieval depths, at 750 MHz and 409 MHz.

it is possible to take advantage of the simplified analytical solution of moisture transfer equation (Sadeghi et al. 2017) such that

$$W'(z, W_0, W_\infty, a) = W_\infty + (W_0 - W_\infty)\exp(z/a), \tag{9}$$

where W_0 is the surface soil moisture, W_∞ is the soil moisture at $z \rightarrow -\infty$, and a is the effective thickness of the capillary edge. To formulate the inverse problem, the time series of TB values were simulated based on the modified Burke model using the measured soil moisture $W_j(z)$ and temperature $T_{s,j}(z)$ profiles for the j^{th} day after irrigation. Herein $Tb_p^{\text{meas}}(\theta, W_j(z), T_{s,j}(z))$ values are referred to as ‘measured’ with modelled values $Tb_p^{\text{mod}}(\theta, W'(z, W_0, W_\infty, a), T_s)$ calculated based on the modified Burke model using the parametric function of the moisture profile in Equations (9). Consequently, the problem of finding the parameters W_0, W_∞, a in the course of minimizing the norm of the discrepancy between the modeled and ‘measured’ values of TBs can be formulated according to

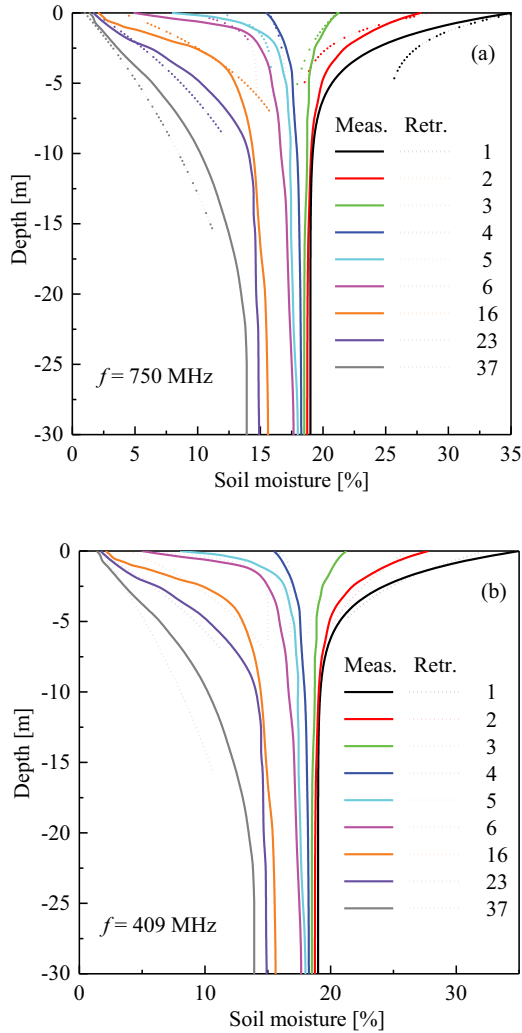


Figure 12. Retrieved and measured soil moisture profiles using simulated TB at 750 MHz and 409 MHz during the 37 days post-irrigation event of [figure 9](#).

$$\{W_0, W_\infty, \alpha\}_j = \min \left\{ \sum_{p, \theta} \left| Tb_p^{\text{mod}}(\theta, W^r, T_s) - Tb_p^{\text{meas}}(\theta, W_j(z), T_{s,j}(z)) \right|^2 \right\}, \quad (10)$$

where T_s is the effective soil temperature calculated with Equation (5), and W^r is the short notation of function $W^r(z, W_0, W_\infty, \alpha)$. Minimization problem (10) was solved similarly to (4) using the Levenberg-Marquardt algorithm (Gill and Murray 1978) simultaneously on both polarizations $p=H, p=V$ in the range of viewing angles from 10° to 50° with step 5° .

Note that Equations (9) and (10) are defined based on the vertical coordinate from 0 m to $-\infty$. From the above analysis (see [Figures 7, 8, and 11](#)), it follows that the thickness of the emitting layer depends on many factors: moisture profile, looking angle, polarization, etc and cannot be calculated or set by any analytical equation (without knowing a priori the moisture profile itself and RCP). At the same time, when calculating $Tb_p^{\text{Burke}}(\theta, W^r, T_s)$, it is

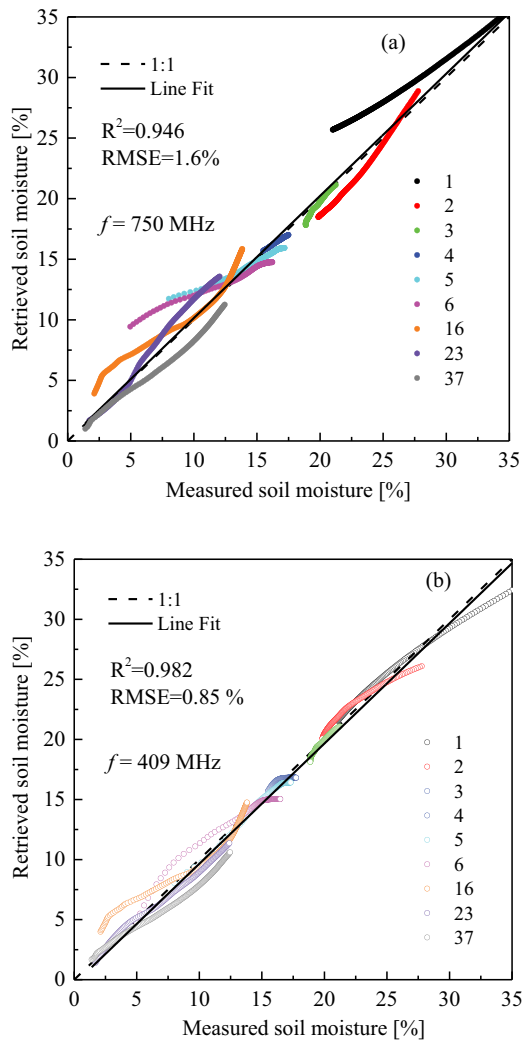


Figure 13. Correlation between retrieved and measured soil moisture profiles using simulated TB at (a) 750 MHz and (b) 409 MHz during the 37 days post-irrigation event in figure 9.

necessary to restrict to a surface soil layer of finite thickness. In this paper, the $Tb_p^{\text{Burke}}(\theta, W^r, T_s)$ was calculated for soil thickness of $l_c = 1/[4k_0\kappa(W)]$, where W is the apparent soil moisture found during minimization of Equation (4). With this approach, the apparent values of W and T_s can always be determined from the measured values of TB.

The layer thickness l_c was calculated at a frequency of 409 MHz and varied from approximately 5 cm to 15 cm. The retrieved moisture profiles at the two frequencies are shown in Figure 12. The correlation between the corresponding retrieved and measured soil moisture values is shown in Figure 13. The error of soil moisture profiles retrieval at 409 MHz is about 2 times smaller (RMSE = 0.85%) than for 750 MHz (RMSE = 1.6%). The main contribution to the overall error in determining soil

moisture profiles at 750 MHz is made by the first few moisturized centimetres of the soil moisture profile (see [Figure 12\(a\)](#)). Accordingly, it can be assumed that if the layer thickness l_c is reduced, the error in soil moisture profiles retrieval can be reduced, and vice versa.

5. Discussion and conclusion

This paper proposed a modified Burke model that was subsequently applied to various soil moisture and temperature profiles (see [Figure 1](#)), showing close agreement of TB calculations between the modified Burke and the coherent Njoku models (see [Figures 2–4](#)), and with experimental measurements ([Figure 5](#)). From a physical perspective, this indicates weak processes of interference of the auxiliary wave, propagating in the soil, with smooth changes in moisture and temperature profiles (see [Figure 1](#)). Similar observations were also described earlier in Newton et al. (1982). It is possible to neglect the phenomena of wave re-reflection in the soil with a similar layered structure (see [Figure 1](#)), which would be essential for the formation of TB. However, between the dielectrically sharp air-soil interface, which is capable of reflecting a substantial amount of wave energy back into the soil, and the permittivity gradients of the underlying soil layers, multiple reflections can take place. Introducing the reflectivity from the surface boundary of layered soil into Equation (1), taking into account phase preservation and multiple re-reflections in the underlying layers using the Brekhovskikh (1960) method, allows this effect to be taken into account. The introduction of coherent reflectivity from air-soil surface in the Burke model made it possible to more accurately consider the influence of the soil moisture profile (but not temperature profile), providing a better match between the modified Burke model and the coherent Njoku model. Accordingly, it follows that the classical incoherent Burke model describes with a sufficient degree of accuracy the influence of the soil temperature profile (see [Figure 1\(b\)](#)) on the brightness temperature.

It was also shown that, due to the influence of the Brewster angle, H-polarization was more than twice as sensitive to changes in soil moisture (4 K/1%) than V-polarization (1.9 K/1%) at a frequency of 750 MHz. This is accompanied by approximately 10 (5) times smaller changes in TB on horizontal (vertical) polarization (see [Figure 6](#)), with varying contrast profiles of physical soil temperature (see [Figure 1\(b\)](#), profiles 1–2) than moisture profiles (see [Figures 6 and 1\(a\)](#), profiles 1–4). A decrease in the polarization index by about 3 times indicates a significant depolarization of the radiation as the soil dries out (see [Figures 6 and 1\(a\)](#), profiles 1 to 4).

In the course of numerical simulations, it was found that the thickness of the emitting layer increased at H-polarization and decreased at V-polarization as the viewing angle increased from nadir (see [Figures 7 and 8](#)). Importantly, the thickness of the emitting layer varies by no more than 10% of the average value (see [Figure 8](#)) when varying temperature profiles from 1 to 2 (see [Figure 1\(b\)](#)). Since the effective temperature very weakly depends on the viewing angle, information about angular dependence of the thickness of the emitting layer is mainly contained in the reflectivity (emissivity). For V-polarization, the reflectivity decreases as the viewing angle increase, which leads to a decrease in the sensitivity of the angular dependence of TB to subsurface layering; for H-polarization, the opposite occurs (note that at probing angles greater than the Brewster angle an increase in probing depth should be observed at V-polarization due to an increase in reflectivity).

Using experimentally measured soil moisture and temperature profiles for 37 days after irrigation, it was shown that the apparent moisture is determined by the emissivity of the soil and only weakly depends on the influence of temperature profile (see Figure 10(b)). Within 37 days after irrigation, the effective soil temperature calculated from the phenomenological radiative transfer model can be predicted by retrieved apparent soil temperatures with an RMSE ~ 0.8 K and a coefficient of determination of at least 0.927 (see Figure 10(a)). In addition, the apparent soil temperature (effective temperature) can be estimated based on the simple analytical formula in Equation (5). The data presented in Figure 10 (solid and short dot lines) and Figure 11 (dash lines) indicate that the integral microwave thermal emission is formed by the much thinner layer of moisture than soil temperature profiles. To explain this phenomenon, the reflective interpretation of microwave emission was used (Rytov 1953; Sharkov 2003, Chapter 4; Tsang, Kong, and Ding 2000, Chapter 5). As noted above the emissivity was mainly responsible for the soil moisture retrieval (see Figure 10(b)). As the soil dried out, the surface layers became more impedance matching layers. The reflection coefficient decreased, and the wave penetrating deeper into the soil, losing less energy and having less energy reflected back from the deep partial layers of the permittivity profile. Consequently, there was a maximum depth of apparent soil moisture retrieval depth l_w (see Figure 11b), which is related to the maximum permittivity gradient (Brekhovskikh 1960; Muzalevskiy 2021), formed between 5 and 10 days after irrigation (see Figure 9(a)). At 30 days after irrigation, when solving the inverse problem using Equation (7) at a frequency of 750 MHz, the apparent soil moisture values W_j turned out to be slightly less than any value of $W_j(z)$. Accordingly, l_w could not be determined, equating to 0 m by the algorithm (see Figure 11(b), red dash line, 30 days after irrigation). In this case, equality between reflectivity from homogeneous moisturized soil with W_j and soil reflectivity with a very smooth moisture profile $W_j(z)$ cannot be achieved for moisture values, which are in the domain of the function $W_j(z)$.

It was also shown that the estimation of emitting thickness layer based on Equation (8) can lead to contradictory results from which it follows that $l_{sd}(f = 750 \text{ MHz}) > l_{sd}(f = 409 \text{ MHz})$ from the 18th day of irrigation (see Figure 11(a)). However, in reality the sensing depth at 750 MHz was less than at 409 MHz. Consequently, the normalized attenuation coefficient calculated using the dielectric model at 750 MHz was less than at 409 MHz (see Figure 11(b), apparent soil moisture at 750 MHz was less than at 409 MHz from 4th day post-irrigation). The classical equation for estimating the thermal skin depth, even with a profile $\kappa_j(z)$ correction (see Equation 8), led to a significant discrepancy with respect to the estimate of l_{Ts} (see Figure 11(a)).

Based on angular, dual-polarization observations of TB, a method was proposed for moisture profile retrieval in the top 5–15 cm layer of soil (depending on surface moisture) using an exponential fitting function, the parameters of which are found in the course of solving the inverse problem. For more complex soil moisture profiles, it is necessary to choose another appropriate regression function. In this case, it was necessary to further estimate the accuracy of the proposed method, which is based on the difference in the thicknesses of the emitting layer depending on the sensing angle and polarization, making it possible to form an overdetermined system of independent nonlinear equations for the minimization problem. For layers of the same thickness, a decrease in the

sensing frequency from 750 MHz to 409 MHz made it possible to increase the accuracy of soil moisture profile retrieval by about 2 times. The conducted studies were carried out for smooth bare soil, which determines the limitations of the method. However, the use of low frequencies of 750 MHz and especially 409 MHz can substantially reduce the effect of soil surface roughness and wave scattering on the elements of vegetation canopy, compared to L-band (Shen et al. 2022a, 2022b; Ye et al. 2021). Both of these factors (roughness and vegetation) reduce reflectivity, which requires separate detailed studies at P-band. Reducing the frequency from 750 MHz to 409 MHz can substantially change the RCP value depending on the texture of wet soil due to the Maxwell-Wagner relaxation processes, which require additional research. The next most significant factor requiring investigation, which can affect the RCP and hence the microwave thermal emission and sensing depth, is the dry bulk density and texture profiles in soil. The use of the Mironov et al. (2013) dielectric model in the modified Burke emission model allowed the layered heterogeneity of soil to be taken into account, not only in terms of volumetric moisture, but also in terms of dry bulk density and clay fraction. Accordingly, the modified Burke emission model had no advantages over previously created models (Brakhasi et al. 2023; E. Njoku and Kong 1977; Shen et al. 2021). However, in general the study confirms the increased depth of soil moisture retrieval at P-band compared to L-band.

Acknowledgements

The work was carried out within the state assignment of Kirensky Institute of Physics and the Australian Research Council funding (DP170102373 and LE150100047) that was used to collect the P-band data.

Disclosure statement

No potential conflict of interest was reported by the author(s).

Funding

The work was supported by the State assignment of Kirensky Institute of Physics [FWES-2021-0034]; Australian Research Council funding [DP170102373 and LE150100047].

References

- Bogorodsky, V. V., and A. I. Kozlov. 1985. *Microwave Radiometry of Earth Surface*, 272. Leningrad: Hydrometeoizdat.
- Brakhasi, F., J. P. Walker, N. Ye, X. Wu, X. Shen, I.-Y. Yeo, N. Boopathi, E. Kim, Y. Kerr, and T. Jackson. 2023. "Towards Soil Moisture Profile Estimation in the Root Zone Using L- and P-Band Radiometer Observations: A Coherent Modelling Approach." *Science of Remote Sensing* 7 (100079): 100079. <https://doi.org/10.1016/j.srs.2023.100079>.
- Brekhovskikh, L. M. 1960. *Waves in Layered Media*, 520. New York/London: Academic Press.
- Burke, W. J., T. J. Schmugge, and J. F. Paris. 1979. "Comparison of 2.8 and 21 Cm Microwave Radiometer Observations Over Soils with Emission Model Calculations." *Journal of Geophysical Research: Atmospheres* 84 (C1): 287–294. <https://doi.org/10.1029/JC084iC01p00287>.
- Chandrasekhar, S. 1950. *Radiative Transfer*, 393. London: Oxford University Press.

- Entekhabi, D., S. Yueh, P. O'Neill, and K. Kellogg. 2014. *SMAP Handbook*, 400–1567. Pasadena, CA, USA: Jet Propulsion Lab.
- Escorihuela, M., A. Chanzy, J. Wigneron, and Y. Kerr. 2010. "Effective Soil Sampling Depth of the L-Band Radiometry: A Case Study." *Remote Sensing of Environment* 114 (5): 995–1001. <https://doi.org/10.1016/j.rse.2009.12.011>.
- Gill, P. E., and W. Murray. 1978. "Algorithms for the Solution of the Nonlinear Least-Squares Problem." *SIAM Journal on Numerical Analysis* 15 (5): 977–992. <https://doi.org/10.1137/0715063>.
- Kerr, Y. H., P. Waldteufel, J. P. Wigneron, J. M. Martinuzzi, J. Font, and M. Berger. 2001. "Soil Moisture Retrieval from Space: The Soil Moisture and Ocean Salinity (SMOS) Mission." *IEEE Transactions on Geoscience and Remote Sensing* 39 (8): 1729–1735. <https://doi.org/10.1109/36.942551>.
- Klepikov, I. N., and E. A. Sharkov. 1983. *Izluchenie Neodnorodnyh Ne Izotermicheskikh Sred [Radiation of Inhomogeneous Non-Isothermal Media]*, 32. Moscow: Preprint, Pr-801, IKI AN SSSR.
- Landau, L. D., and E. M. Lifshitz. 1960. *Electrodynamics of Continuous Media*, 400. London: Pergamon Press.
- Liu, P. W., R. D. D. Roo, A. W. England, and J. Judge. 2013. "Impact of Moisture Distribution within the Sensing Depth on L- and C-Band Emission in Sandy Soils." *IEEE Journal of Selected Topics in Applied Earth Observations & Remote Sensing* 6 (2): 887–899. <https://doi.org/10.1109/JSTARS.2012.2213239>.
- Mironov, L., P. P. Bobrov, and S. V. Fomin. 2013. "Dielectric Model of Moist Soils with Varying Clay Content in the 0.04 to 26.5 GHz Frequency Range." *International Siberian Conference on Control and Communications (SIBCON)*, Krasnoyarsk, Russia, 1–4.
- Mironov, V. L., A. Y. Karavayskiy, Y. I. Lukin, and I. P. Molostov. 2020. "A Dielectric Model of Thawed and Frozen Arctic Soils Considering Frequency, Temperature, Texture and Dry Density." *International Journal of Remote Sensing* 41 (10): 3845–3865. <https://doi.org/10.1080/01431161.2019.1708506>.
- Muzalevskiy, K. 2021. "Retrieving Soil Moisture Profiles Based on Multifrequency Polarimetric Radar Backscattering Observations. Theoretical Case Study." *International Journal of Remote Sensing* 42 (2): 506–519. <https://doi.org/10.1080/01431161.2020.1809743>.
- Newton, R. W., Q. R. Black, S. Mankanvand, A. J. Blanchard, and B. R. Jean. 1982. "Soil Moisture Information and Thermal Microwave Emission." *IEEE Transactions on Geoscience & Remote Sensing* GE-20 (3): 275–281. <https://doi.org/10.1109/TGRS.1982.350443>.
- Njoku, E., and J. A. Kong. 1977. "Theory for Passive Microwave Remote Sensing of Near-Surface Soil Moisture." *Journal of Geophysical Research* 82 (20): 3108–3118. <https://doi.org/10.1029/JB082i020p03108>.
- Njoku, E. G., J. Schiedge, and A. B. Kahle. 1980. *Joint Microwave and Infrared Studies for Soil Moisture Determination*, 130. Pasadena: Jet Propulsion Laboratory.
- Rytov, S. 1953. *The Theory of Electrical Fluctuations and Thermal Radiation*. Moscow: U.S.S.R. Academy of Sciences, U.S. Air Force Cambridge Research Center, Bedford, Massachusetts, Rep. AFCRC-TR -59-162.
- Sadeghi, M., A. Tabatabaenejad, M. Tuller, M. Moghaddam, and S. B. Jones. 2017. "Advancing Nasa's AirMOSS P-Band Radar Root Zone Soil Moisture Retrieval Algorithm via Incorporation of Richards' Equation." *Remote Sensing* 9 (1): 1–17. <https://doi.org/10.3390/rs9010017>.
- Schmugge, T. 1980. *Effect of Soil Texture on the Microwave Emission from Soils*, 32. Vols. TM-80632. Greenbelt, Maryland: NASA, Goddard space flight center.
- Schmugge, T., W. Wilheit, J. Webster, and P. Gloersen. 1976. "Remote Sensing of Soil Moisture with Microwave Radiometers-II." NASA technical note D-8321: 34.
- Schrnugge, T. J., and B. J. Choudhury. 1981. "A Comparison of Radiative Transfer Models for Predicting the Microwave Emission from Soils." *Radio Science* 16 (5): 927–938. <https://doi.org/10.1029/RS016i005p00927>.
- Sharkov, E. A. 2003. *Passive Microwave Remote Sensing of the Earth*, 613. Berlin, Heidelberg: Springer.
- Shen, X., J. P. Walker, N. Ye, X. Wu, N. Boopathi, I.-Y. Yeo, L. Zhang, et al. 2021. "Soil Moisture Retrieval Depth of P- and L-Band Radiometry: Predictions and Observations." *IEEE Transactions on Geoscience and Remote Sensing* 59 (8): 6814–6822. <https://doi.org/10.1109/TGRS.2020.3026384>.

- Shen, X., J. P. Walker, N. Ye, X. Wu, F. Brakhasi, N. Boopathi, L. Zhu, et al. 2022a. "Evaluation of the Tau-Omega Model Over Bare and Wheat-Covered Flat and Periodic Soil Surfaces at P- and L-Band." *Remote Sensing of Environment* 273 (112960): 112960. <https://doi.org/10.1016/j.rse.2022.112960>.
- Shen, X., J. P. Walker, N. Ye, X. Wu, F. Brakhasi, N. Boopathi, L. Zhu, et al. 2022b. "Impact of Random and Periodic Surface Roughness on P- and L-Band Radiometry." *Remote Sensing of Environment* 269 (112825): 112825. <https://doi.org/10.1016/j.rse.2021.112825>.
- Shulgina, E. M. 1975. "Radioizluchenie vertikal'no-neodnorodnoj sredy [Radio emission of a vertically inhomogeneous medium]." *Proceedings of Voeikov Main Geophysical Observatory*. 331: 64–72.
- Stogryn, A. 1970. "The Brightness Temperature of a Vertically Structured Medium." *Radio Science* 5 (12): 1397–1406. <https://doi.org/10.1029/RS005i012p01397>.
- Tsang, L., and J. A. Kong. 1975. "The Brightness Temperature of a Half-Space Random Medium with Nonuniform Temperature Profile." *Radio Science* 10 (12): 1025–1033. <https://doi.org/10.1029/RS010i012p01025>.
- Tsang, L., J. Kong, and K. Ding. 2000. *Scattering of Electromagnetic Waves: Theories and Applications*. New York: Wiley-Interscience.
- Tsang, L., E. Njoku, and J. A. Kong. 1975. "Microwave Thermal Emission from a Stratified Medium with Nonuniform Temperature Distribution." *Journal of Applied Physics* 46 (12): 5127–5133. <https://doi.org/10.1063/1.321571>.
- Ulaby, F. T., D. G. Long, W. J. Blackwell, C. Elachi, A. K. Fung, C. Ruf, K. Sarabandi, H. A. Zebker, and J. Van Zyl. 2014. *Microwave Radar and Radiometric Remote Sensing*, 1013. Ann Arbor: University of Michigan Press.
- Wang, J. R., and B. J. Choudhury. 1980. *Remote Sensing of Soil Moisture Content Over Bare Fields at 1.4 GHz Frequency*, 27. Greenbelt, Maryland: NASA, Goddard space flight center.
- Wang, J. R., and T. J. Schmugge. 1980. "An Empirical Model for the Complex Dielectric Permittivity of Soils as a Function of Water Content." *IEEE Transactions on Geoscience & Remote Sensing* GE-18 (4): 288–295. <https://doi.org/10.1109/TGRS.1980.350304>.
- Wilheit, T. T. 1978. "Radiative transfer in a plane stratified dielectric." *IEEE Transactions on Geoscience Electronics* 16 (2): 138–143. <https://doi.org/10.1109/TGE.1978.294577>.
- Ye, N., J. P. Walker, I.-Y. Yeo, T. J. Jackson, Y. Kerr, E. Kim, A. Mcgrath, et al. 2021. "Toward P-Band Passive Microwave Sensing of Soil Moisture." *IEEE Geoscience and Remote Sensing Letters* 18 (3): 504–508. <https://doi.org/10.1109/LGRS.2020.2976204>.